Plasma property investigations during negative ion beam extraction in a half-sized ITER NBI ion source at ELISE test facility

D. Yordanov, D. Wünderlich, R. Riedl, C. Wimmer, A. Heiler, A. Döring, Ursel Fantz

Angaben zur Veröffentlichung / Publication details:

Yordanov, D., D. Wünderlich, R. Riedl, C. Wimmer, A. Heiler, A. Döring, and Ursel Fantz. 2025. "Plasma property investigations during negative ion beam extraction in a half-sized ITER NBI ion source at ELISE test facility." Fusion Engineering and Design 217: 115130. https://doi.org/10.1016/j.fusengdes.2025.115130.

Fusion Engineering and Design 217 (2025) 115130

Contents lists available at ScienceDirect

Fusion Engineering and Design

journal homepage: www.elsevier.com/locate/fusengdes

Plasma property investigations during negative ion beam extraction in a half-sized ITER NBI ion source at ELISE test facility

D. Yordanov [a,*], D. Wünderlich [a], R. Riedl [a], C. Wimmer [a], A. Heiler [a], A. Döring [a], U. Fantz [a,b]

[a] Max–Planck-Institut für Plasmaphysik, Boltzmannstr. 2, Garching, 85748, Germany
[b] AG Experimentelle Plasmaphysik, Universität Augsburg, Augsburg, 86135, Germany

ARTICLE INFO

Keywords:
ELISE negative ion source
CW extraction
Plasma diagnostics
Co-extracted electrons
Langmuir probe
Optical emission spectroscopy
Tunable diode laser absorption

ABSTRACT

The RF negative hydrogen/deuterium ion source at the ELISE test facility is half the size of the ITER negative ion source for neutral beam injection (NBI). ELISE demonstrated 90 % of the ITER NBI requirement for the extracted negative ion current density in hydrogen for 600 s pulse for the first time, limited only by the available RF power. However, the electrons inevitably co-extracted with the negative ions increase in time and can limit the source performance. The majority of the extracted negative ions are surface produced by the conversion of atoms and positive ions on low-work function surfaces, achieved by cesium evaporation in the ion source. The temporal increase in the co-extracted electrons is associated with the cesium dynamics during long pulses close to the extraction region. This motivates a detailed investigation of the temporal behavior of the cesium and the effect on the plasma parameters and the co-extracted electrons at ELISE. For this purpose, a Langmuir probe, optical emission spectroscopy and tunable diode laser absorption are used to resolve plasma properties over the pulse length and correlate them with the co-extracted electron current density. It is shown that the cesium density decreases at the beginning of the pulse, which causes a change in the plasma potential structure in front of the extraction region, resulting in an increase of the co-extracted electrons. Stabilizing the co-extracted electrons can be achieved by varying the temperatures of the plasma grid and the bias plate which sustain a low value of the work function, resulting in a smaller slope of the co-extracted electrons' temporal increase.

1. Introduction

The neutral beam injection (NBI) is an essential heating system for ITER [1]. Two injectors are planned initially to be installed, delivering 16.6 MW each, and a third one is under consideration. The required beam energy is either 1 MeV up to one hour in deuterium or 0.87 MeV up to several hundred seconds in hydrogen. At these high energies, the neutralization efficiency of the hydrogen/deuterium positive ions drops below 5 % [3], while of the negative ions remains ~ 60 %, therefore, the use of a negative ion source is mandatory. ITER requires accelerated current densities of 230 Am^{-2} for hydrogen and pulse length up to several hundred seconds and 200 Am^{-2} for up to one hour in deuterium. Considering stripping losses of 30 % [4] in the accelerator grids at 0.3 Pa filling pressure results in required extracted negative ion current densities of 329 Am^{-2} and of 286 Am^{-2} for hydrogen and for deuterium respectively. The extraction of negative ions is accompanied by the co-extraction of electrons, which are deflected from the beam via a magnetic field, produced by embedded magnets in the second grid (extraction grid — EG) of the extraction system and then collected

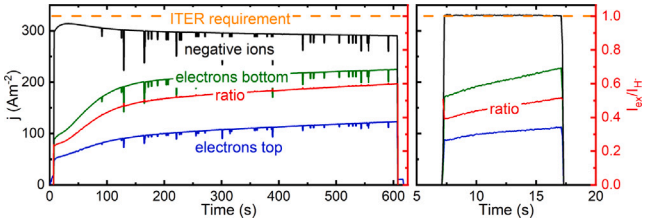

Fig. 1. Time traces of the extracted negative ion current density, the co-extracted electron current density and their current ratio for the best 600 s pulse (left-hand side plot) and short 10 s pulse (right-hand side plot) in hydrogen at ELISE [2].

* Corresponding author.
E-mail address: dimitar.yordanov@ipp.mpg.de (D. Yordanov).

https://doi.org/10.1016/j.fusengdes.2025.115130
Received 16 January 2025; Received in revised form 25 March 2025; Accepted 24 April 2025
Available online 15 May 2025

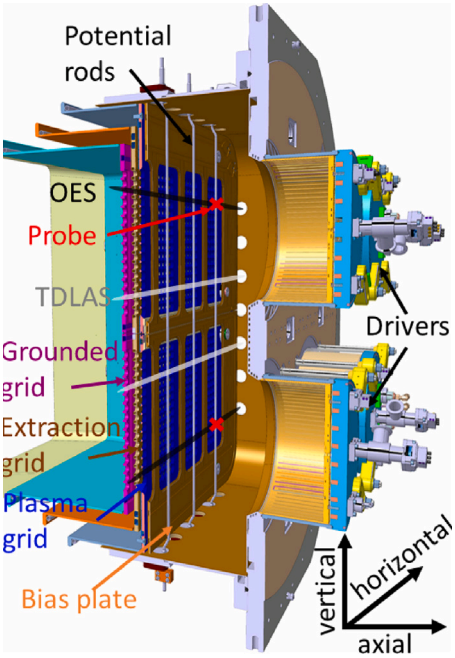

Fig. 2. CAD drawing of ELISE ion source with an illustration of the location of the used diagnostics in the study.

by the EG. The electron heat load must remain low, therefore, to avoid damage to the grid, the co-extracted electron to the negative ion current ratio (I_{ex}/I_{H-}) is allowed to be one at the maximum.

The negative ion source at the ELISE (Extraction from a Large Ion Source Experiment) test facility [5] is half the size of the ITER ion source. It is an important step in the ion source development, aiming to demonstrate the ITER requirements for the extracted current densities. In fact, ELISE has shown the capability to produce (Fig. 1) 90 % for 600 s of the extracted hydrogen negative ion current density required for ITER and has achieved the requirement for short (10 s) pulses [2]. These results were obtained with the maximum available RF power at ELISE of 75 kW per driver, while for the ITER ion source 100 kW per driver is foreseen. As it can be seen from Fig. 1 the main challenge is the increase of the co-extracted electrons current density (j_e) over time, which can reach the power limit of the EG, particularly in deuterium. This study aims namely to investigate the plasma properties in the vicinity of the extraction region, which can affect the co-extracted electron current and its temporal behavior. The investigations are done in hydrogen.

2. The ELISE test facility

The ELISE ion source (Fig. 2) has 4 cylindrical drivers, where the discharge is generated by inductive RF coupling (1 MHz) in each driver (up to 75 kW). The plasma expands in a common chamber for all drivers towards the extraction system. Since the main process for the production of negative ions is the conversion of atoms and positive ions on a low work function surface [6], the ion source is equipped with two cesium ovens (on the right and the left side in the expansion), delivering cesium into the source to provide a low work function on the first grid of the extraction system. The negative ions and the electrons are extracted by a three grid system, consisting of 640 apertures arranged in 8 beamlet groups. The first is the plasma grid (PG) in contact with the plasma, the second is the EG and the acceleration grid (AG) is the third one. An extraction potential up to 12 kV is applied on the first gap between the PG and EG, and an acceleration voltage up to 50 kV is applied in the second gap between the EG and AG. A window frame structured bias plate (BP), electrically isolated, covers the area between the beamlet groups and it is positioned 7 mm away from the PG. A high current flows through the PG and splits up to different return conductors, resulting in a magnetic filter field (FF) with a maximum strength of a few milli Tesla for suppression of the co-extracted electrons and the reduction of electron temperature close to the extraction region. Changing the current through the return conductors can change the magnetic field topology. The results in the study are with FF topology similar to the one used at MITICA test facility [7,8], which is of high relevance for ITER. However, applying a magnetic FF results in vertical plasma inhomogeneity caused by $\mathbf{E} \times \mathbf{B}$ and diamagnetic plasma drifts [9,10]. In the standard source operation, the high-current flows from bottom to top through the PG, resulting in an effective drift-up. The vertical plasma asymmetry of the spatial and temporal (within the RF cycle) plasma potential, electron density and temperature distribution affect j_e and can lead to high local heat load deposition on the EG. Biasing the PG [11] and letting the BP on a floating potential [12,13] change the potential difference (between plasma and PG or BP potentials) in the vicinity of the extraction region. This provides an electron attracting region towards PG or BP (Fig. 3), resulting in a collection of the plasma electrons to the surface before extraction and it reduces j_e. However, this is a static effect and does not solve the temporal behavior of j_e during extraction.

All walls including the extraction system grids are equipped with water cooling/heating systems, allowing to set the surface temperatures before source operation. However, it is found that actively increasing the temperatures of the PG (T_{PG}) and BP (T_{BP}) (from 110 °C to 160 °C, with an increase rate depending on the heater power and the plasma source parameters) during the pulse stabilize the temporal increase of the co-extracted electrons. In fact, with this procedure is achieved the result presented in Fig. 1. This effect will be discussed in more detail in the next section. In addition, the experiments in the study are performed with the so-called potential rods, which are on floating potential and positioned in a vertical direction between the beamlet groups [14], providing improved top/bottom symmetry of the co-extracted electrons.

To understand the underlying physics processes and further optimization of the ion source, ELISE is equipped with a variety of plasma and beam diagnostics as well as current measurements. The study focuses on the results of the temporal behavior and the vertical inhomogeneity of j_e and its correlation with the plasma properties. The EG is divided by top and bottom segments which are electrically isolated, allowing to measure j_e simultaneously on each segment. For the purpose of plasma diagnostics in the expansion region of the source are in use two cylindrical RF compensated Langmuir probes (LP) [15], measuring electron density (n_e), electron temperature (T_e) and the plasma potential (U_{pl}), optical emission spectroscopy (OES) [16] for n_e and T_e, and tunable diode laser absorption spectroscopy (TDLAS) [17] for neutral cesium density (n_{cs}). The axial position of the probes and the line of sights (LOS) of OES and TDLAS are located 2 cm upstream of the PG on the top and bottom part of the source as indicated in Fig. 2. The Langmuir probes provide results from local measurements, while OES and TDLAS results are averaged over the LOS.

3. Results and discussions

The investigations in the study are conducted at ion source parameters required for ITER, which ELISE can provide, i.e. hydrogen discharge at 0.3 Pa, an extraction pulse length of 600 s and MITICA-like topology of the magnetic FF (1.4 mT in the region of the measurements [7]). The maximum available RF power of 75 kW per driver is used. ELISE is not equipped with the full acceleration beam system required for ITER, however, the extraction voltage in the first gap of 10.5 kV and the acceleration voltage in the second gap of 30 kV are used. The PG is biased with a current source set to $I_{bias} = 1$ A, providing a PG potential (U_{PG}) between 26 V and 29 V and the BP is let on a

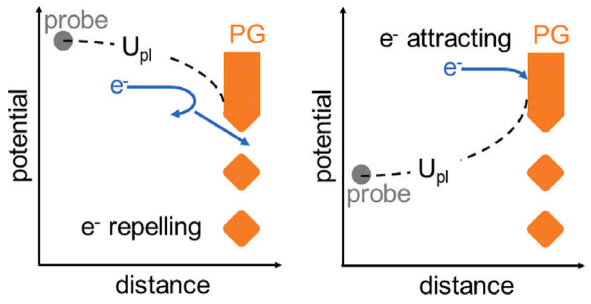

Fig. 3. Schematic representation of electron attracting and repelling regions. This representation does not include the plasma sheath on the PG surface, only the plasma and wall potentials difference.

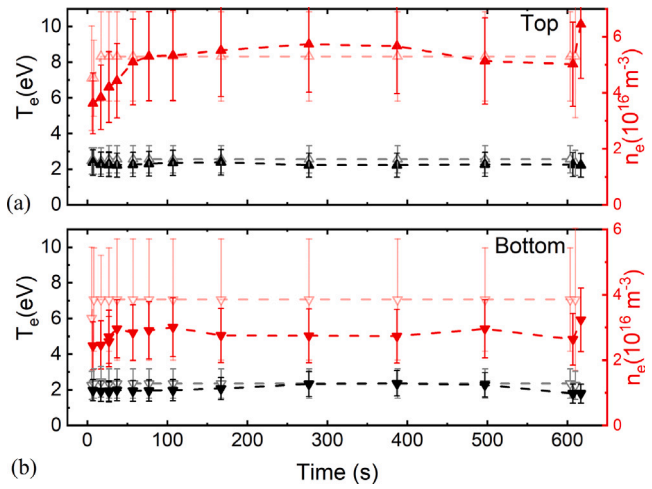

Fig. 4. The change of T_e in black and n_e in red along the extraction pulse measured with LP the full symbols and OES the open symbols on top (a) and bottom (b) parts of the source.

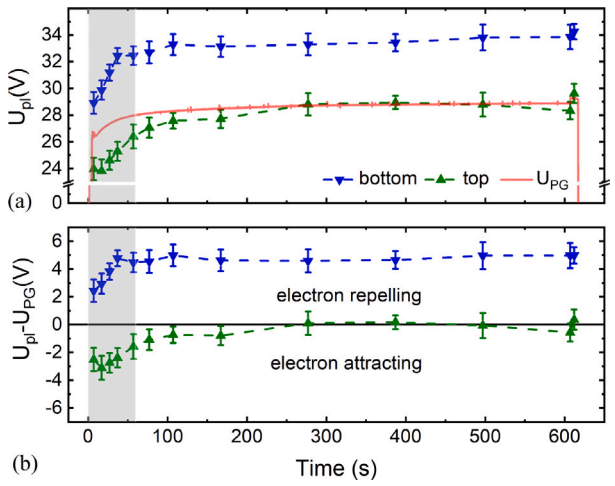

Fig. 5. The change of U_{pl} on top (the green symbols) and bottom (the blue symbols) and U_{PG} (the red curve) (a) and the potential difference $U_{pl} - U_{PG}$ on top and bottom (b) during the extraction pulse.

floating potential. The results for the plasma diagnostics below are for the same long pulse presented in Fig. 1.

Since the plasma parameters and extracted currents dynamic is stronger in the first 100 s of the pulse (Fig. 1) the Langmuir probes receive triggers more often at the beginning of the pulse. After that, the measurements are in every 100 s with one last measurement when the extraction is off, but the discharge is still on. The electron temperature and density (Fig. 4 the full symbols) as well as plasma potential (Fig. 5(a)) results obtained from LP are evaluated by using the methods described in [15] with the corresponding uncertainties. The optical emission spectroscopy results (Fig. 4 the open symbols) are measured at the same time when the Langmuir probes get triggered. The intensities of H_α, H_β, and H_γ lines are recorded and used as input parameters in the collisional radiative model Yacora [18] to obtain n_e and T_e. The measurements are in the expansion region of the source, which is characterized by a plasma with dominance of the recombination processes [19]. Therefore, to evaluate n_e and T_e must be used an assumption for the unknown particle densities of the hydrogen molecules, positive (H^+, H_2^+ and H_3^+ with relative ratio 40%/40%/20%, respectively) and negative ions, considering the quasi-neutrality of the plasma. Since T_e is suppressed to below 2 eV via FF in the extraction region, the recombination of the negative hydrogen ions with the atomic positive ions can affect the Balmer emission lines, in particular H_α, which could lead to increased uncertainty of the OES measurements. However, OES results agree surprisingly well with those from the LP diagnostics. Discussion on the uncertainties in the plasma diagnostic methods is not in the scope of the present study.

The electron density and the plasma potential are vertically inhomogeneous due to the ×**B** drifts – n_e is higher on top (Fig. 4), where U_{pl} has lower values (Fig. 5(a)). The electron temperature is vertically symmetric and does not change during the pulse, remaining ~ 2 eV. The biggest temporal change of n_e is in the first 60 s of the pulse, where on top it increases more pronounced — from 3.6×10^{16} m^{-3} to 5.3×10^{16} m^{-3} (i.e. by 50%) whereas on bottom from 2.4×10^{16} m^{-3} to 3×10^{16} m^{-3} (i.e. by 25%). The plasma potential (Fig. 5(a)) on the bottom changes from 28.9 V to 33.3 V and after that is almost constant — a slight increase of 0.5 V within the error bars. On top U_{pl} increases from 23.8 V to 27.6 V in the first 100 s of the pulse. After that, it continues to increase with a local maximum of 29.1 V at 400 s and decreases to 28.3 V at the end of the pulse. Since, U_{PG} is set via a current source, it is self-adjusting to the local plasma parameters: n_e and U_{pl} changes within the pulse length, U_{PG} changes as well. Comparing U_{PG} with the local U_{pl} determines whether the PG attracts or repels electrons.

The temporal results for $U_{pl} - U_{PG}$ (Fig. 5(b)) correlate with those for j_e (Fig. 6(a)): $U_{pl} - U_{PG} > 0$ V on the bottom part of the source, creating an electron-repelling sheath where the electrons remain in the discharge in the vicinity of the extraction apertures and are ready to be extracted. On top, however, $U_{pl} - U_{PG} \leq 0$ V indicates an electron- attracting sheath (Fig. 3), resulting in an increased collection of electrons on the PG surface before the extraction and it provides smaller j_e regardless of higher n_e (Fig. 4) in this region. The PG surface collects the majority of the plasma electrons and less are extracted. Therefore, the main factor determining j_e is the potential difference $U_{pl} - U_{PG}$, not n_e. The change of $U_{pl} - U_{PG}$ from 2 V to 5 V in the first 60 s on bottom increases the potential barrier of the electron flux towards the PG surface, resulting in a strong rise of j_e — from 90 Am^{-2} to 190 Am^{-2} in the beginning of the pulse. While on top $U_{pl} - U_{PG}$ changes from −3.5 V to ~ 0 V and the increase of j_e is not that well steep — from 51 Am^{-2} to 95 Am^{-2}. Since U_{PG} rises monotonously from 26.5 V to 28.9 V during the pulse, the changes of U_{pl} determines the temporal dynamics of the potential difference, particularly at the beginning of the pulse — in the first 100 s.

It is known that cesium and the negative ions can affect the plasma potential [15,20]. Fig. 6(b) shows the dynamics of n_{cs} during the pulse, starting with a strong decrease in the first 60 s – from 3×10^{14} m^{-3} to below 1.5×10^{14} m^{-3} – with a similar inverse trend as the initial increase in U_{pl}, particularly on the bottom. After the first 60 s of the pulse n_{cs} and U_{pl} almost does not change until the end of the pulse on the bottom side of the source. On the top, however, after 350 s n_{cs} increases to 2.3×10^{14}

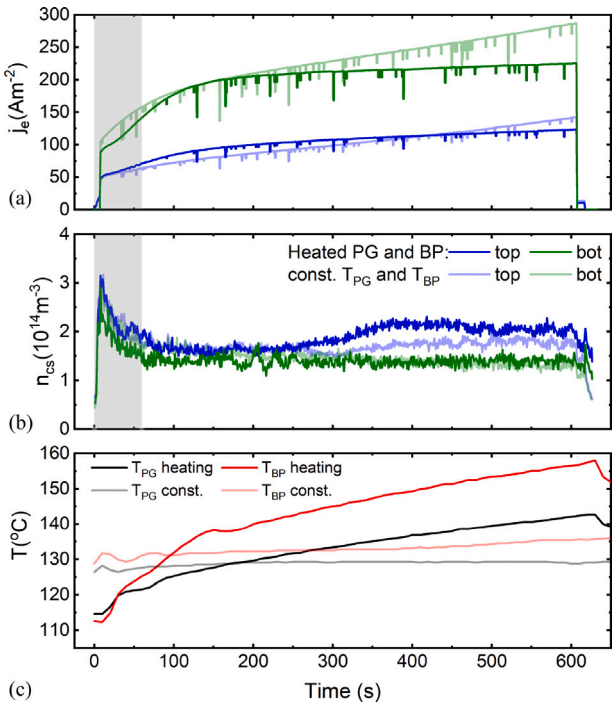

Fig. 6. Comparison of pulses with constant temperatures and increasing temperatures of PG and BP during extraction pulses: temperature profiles of PG and BP (a), the change of n_{cs} on top and bottom (b) and the change of j_e on top and bottom (c). The results with increasing temperatures of PG and BP are for the same pulse as the results presented in Figs. 4 and 5.

m^{-3}, affecting U_{pl} as well (Fig. 5) — a maximum of 29.1 V at ~ 400 s with a decrease until the end of the pulse 28.3 V.

Cesium ensures the low work function on the PG and the BP, however, experiments in smaller set up at similar vacuum conditions as at ELISE [21] show that a small amount of impurities (mostly oxygen) in the cesium layer provides a work function below 1.4 eV which is surface temperature dependent. This motivates an investigation of the T_{PG} and T_{BP} effect on j_e and n_{cs}. Fig. 6 shows the comparison of two long pulses with the same source parameters, one with constant T_{PG} and T_{BP} ~ 130 °C (Fig. 6(c) the transparent curves) and one with increasing T_{PG} and T_{BP} as shown in Fig. 6(c) the non-transparent curves. From the n_{cs} dynamics (Fig. 6(b)) is clear that at the beginning of the pulse, there is no difference in both cases. In the second part of the pulse after 300 s T_{PG} > 130 °C and T_{BP} > 145 °C, n_{cs} starts to increase on top, due to the rising evaporation of cesium from the PG and BP. The temperature effect on j_e (Fig. 6(a)) is a reduction of the increase rate of the co-extracted electrons at the end of the pulse and a smaller slope after the initial rise (until 150 s), particularly on the bottom side of the source. The working hypothesis of the n_{cs} increase on top and the reduction of j_e increase rate on the bottom is due to the inhomogeneity of U_{pl}, n_e and change of the work function. During the vacuum phase (5 to 10 min) before the pulse, more n_{cs} is accumulated on top, which is an effect of the pulse prior to the vacuum phase — the neutral cesium condenses on the walls at the end of the pulse. During the pulse presented in Fig. 6 with T_{PG} and T_{BP} increase, the cesium is released from the surfaces, after that positively ionized and redistributed towards the bottom side of the source during the pulse where it "sees" an attractive electric field ($U_{pl} - U_{PG} > 0$ V) towards the PG. The cesium redistribution effect together with the change of the work function favors j_e on the bottom part of the source. However, this effect cannot be seen in n_{cs} dynamics, since TDLAS measures only the neutral cesium density and work function measurements are not installed at ELISE. Nevertheless, the increasing T_{PG} and T_{BP} in the course of the pulse stabilize j_e and help to achieve the long pulse presented in Fig. 1.

4. Summary

The ion source at the ELISE test facility has demonstrated that the extracted negative ion current density required for the DT-1 phase scenario of ITER operation can be fulfilled, by achieving ~ 90% with the maximum available RF power 75 kW per driver, while the ITER ion source will be equipped with generators capable of delivering 100 kW per driver. A critical point is the co-extracted electrons. Their temporal increase along the pulse and the vertical inhomogeneity can limit the source performance.

The potential structure in front of the extraction region has a major role for the behavior of j_e: $U_{pl} - U_{PG}$ is below 0 V on top and it defines an electron-attracting region, resulting in a collection of electrons on PG and lower j_e regardless of the higher n_e in this region. On bottom is an electron-repelling sheath with positive $U_{pl} - U_{PG}$, where the electrons remain in the plasma and are extracted more likely, causing higher j_e. The temporal behavior of j_e shows a strong increase in the first 100 s of the pulse, particularly on bottom, related to the n_{cs} decrease. Lower n_{cs} provides higher U_{pl} and respectively $U_{pl} - U_{PG}$ allowing more electrons being co-extracted. Therefore, the co-extracted electron current density is a strong interplay between potential and cesium distribution in the vicinity of the extraction. However, increasing PG and BP temperatures along the pulse stabilizes co-extracted electrons by providing a temporal increase of j_e with a smaller slope, due to cesium redistribution. An option for further optimization of co-extracted electrons particularly in deuterium would be improved cesium delivery in the extraction region such as a cesium shower [22].

CRediT authorship contribution statement

D. Yordanov: Writing – review & editing, Writing – original draft, Visualization, Validation, Investigation, Formal analysis, Data curation, Conceptualization. **D. Wünderlich:** Writing – review & editing, Investigation, Formal analysis. **R. Riedl:** Investigation. **C. Wimmer:** Writing – review & editing. **A. Heiler:** Writing – review & editing. **A. Döring:** Writing – review & editing, Investigation, Conceptualization. **U. Fantz:** Writing – review & editing, Project administration, Funding acquisition, Conceptualization.

Declaration of competing interest

The authors declare that they have no known competing financial interests or personal relationships that could have appeared to influence the work reported in this paper.

Acknowledgments

This work has been carried out within the framework of the EUROfusion Consortium, funded by the European Union via the Euratom Research and Training Programme (Grant Agreement No 101052200 — EUROfusion). Views and opinions expressed are however those of the author(s) only and do not necessarily reflect those of the European Union or the European Commission. Neither the European Union nor the European Commission can be held responsible for them.

Data availability

Data will be made available on request.

References

[1] R.S. Hemsworth, et al., Overview of the design of the ITER heating neutral beam injectors, New J. Phys. 19 (2) (2017) 025005.

[2] D. Wünderlich, R. Riedl, M. Fröschle, A. Heiler, A. Navarro, D. Yordanov, A. Döring, U. Fantz, ITER-relevant 600 s steady-state extraction of negative hydrogen ions at the test facility ELISE, Nucl. Fusion 65 (1) (2025) 014001.

[3] K.H. Berkner, R.V Pyle, J.W Stearns, Intense, mixed-energy hydrogen beams for CTR injection, Nucl. Fusion 15 (2) (1975) 249.

[4] A. Krylov, R.S. Hemsworth, Gas flow and related beam losses in the ITER neutral beam injector, Fusion Eng. Des. 81 (19) (2006) 2239–2248.

[5] B. Heinemann, et al., Towards large and powerful radio frequency driven negative ion sources for fusion, New J. Phys. 19 (1) (2017) 015001.

[6] D Wünderlich, L Schiesko, P McNeely, U Fantz, P Franzen, the NNBI-Team, On the proton flux toward the plasma grid in a RF-driven negative hydrogen ion source for ITER NBI, Plasma Phys. Control. Fusion 54 (12) (2012) 125002.

[7] G. Chitarin, P. Agostinetti, D. Aprile, N. Marconato, P. Veltri, Improvements of the magnetic field design for SPIDER and MITICA negative ion beam sources, AIP Conf. Proc. 1655 (1) (2015) 040008.

[8] D Wünderlich, W Kraus, M Fröschle, R Riedl, U Fantz, B Heinemann, the NNBI team, Influence of the magnetic field topology on the performance of the large area negative hydrogen ion source test facility ELISE, Plasma Phys. Control. Fusion 58 (12) (2016) 125005.

[9] S Lishev, L Schiesko, D Wünderlich, C Wimmer, U Fantz, Fluid-model analysis on discharge structuring in the RF-driven prototype ion-source for ITER NBI, Plasma Sources Sci. Technol. 27 (12) (2018) 125008.

[10] U. Fantz, L. Schiesko, D. Wünderlich, Plasma expansion across a transverse magnetic field in a negative hydrogen ion source for fusion, Plasma Sources Sci. Technol. 23 (4) (2014) 044002.

[11] Christian Wimmer, Ursel Fantz, Extraction of negative charges from an ion source: Transition from an electron repelling to an electron attracting plasma close to the extraction surface, J. Appl. Phys. 120 (7) (2016) 073301.

[12] D. Yordanov, D. Wünderlich, C. Wimmer, U. Fantz, On the effect of biased surfaces in the vicinity of the large extraction area of the ELISE test facility, J. Phys.: Conf. Ser. 2244 (1) (2022) 012050.

[13] U Fantz, S Briefi, M Fröschle, N den Harder, A Heiler, B Heinemann, A Hurlbatt, C Hopf, M Lindqvist, F Merk, A Mimo, R Nocentini, G Orozco, R Riedl, G Starnella, C Wimmer, D Wünderlich, D Yordanov, D Zielke, Ion source developments at IPP: On the road towards achieving the ITER-NBI targets and preparing concepts for DEMO, J. Phys.: Conf. Ser. 2244 (1) (2022) 012049.

[14] D. Wünderlich, C. Wimmer, N. den Harder, M. Barnes, M. Fröschle, A. Heiler, A. Navarro, R. Riedl, D. Yordanov, U. Fantz, B. Heinemann, the NNBI Team, Towards ITER-Relevant CW Extraction at Negative Ion Sources for Fusion, J. Phys.: Conf. Ser. 2743 (1) (2024) 012026.

[15] P McNeely, S V Dudin, S Christ-Koch, U Fantz, the NNBI Team, A Langmuir probe system for high power RF-driven negative ion sources on high potential, Plasma Sources Sci. Technol. 18 (1) (2008) 014011.

[16] D. Wünderlich, U. Fantz, P. Franzen, R. Riedl, F. Bonomo, Optical emission spectroscopy at the large RF driven negative ion test facility ELISE: Instrumental setup and first results, Rev. Sci. Instrum. 84 (9) (2013) 093102.

[17] U. Fantz, C. Wimmer, Optimizing the laser absorption technique for quantification of caesium densities in negative hydrogen ion sources, J. Phys. D: Appl. Phys. 44 (33) (2011) 335202.

[18] D. Wünderlich, M. Giacomin, R. Ritz, U. Fantz, Yacora on the web: Online collisional radiative models for plasmas containing h, H2 or he, J. Quant. Spectrosc. Radiat. Transfer 240 (2020) 106695.

[19] Dirk Wünderlich, Ursel Fantz, Evaluation of State-Resolved Reaction Probabilities and Their Application in Population Models for He, H, and H2, Atoms 4 (4) (2016).

[20] D. Yordanov, D. Wünderlich, C. Wimmer, R. Riedl, A. Navarro, U. Fantz, the NNBI Team, Plasma homogeneity over the extraction beamlet groups at the half size ITER negative ion source at ELISE test facility, J. Phys.: Conf. Ser. 2743 (1) (2024) 012034.

[21] A. Heiler, Influence of Particle and Photon Fluxes of Hydrogen Plasmas on the Work Function of Caesiated Surfaces, Ph.D. thesis University of Augsburg, 2022.

[22] C. Wimmer, A. Döring, T. Fellinger, M. Fröschle, A. Heiler, D. Mussini, U. Fantz, Stabilizing long pulse deuterium extraction for NBI using a Cs shower, Fusion Eng. Des. 215 (2025) 114949.